EFFECTS OF ALLOYING SUBSTRATES ON THE CHARACTERISTICS OF THE LITHIUM NEGATIVE ELECTRODE

MASAYUKI MORITA* and YOSHIHARU MATSUDA

Department of Industrial Chemistry, Faculty of Engineering, Yamaguchi University, Tokiwadai, Ube 755 (Japan)

Summary

Amorphous alloys of $Ni_{70}Al_{10}B_{20}$ and $Co_{70}Al_{10}B_{20}$ have been used as negative electrode substrates for rechargeable lithium batteries. The charge–discharge behavior of lithium has been investigated at the alloy substrates in some organic electrolytes. The highest cycling efficiency was observed at the amorphous $Co_{70}Al_{10}B_{20}$ substrate in a mixture of dimethylsulfoxide and propylene carbonate containing $LiPF_6$. The cycling efficiency of this type of substrate depended on the diffusion coefficient of lithium in the alloy as well as on the exchange current for lithium deposition from the organic solution.

Introduction

Alloy electrodes consisting of lithium with aluminium or Wood's metal (fusible metals) can be used in long cycle life rechargeable lithium batteries operated at room temperature [1 - 4]. A negative electrode substrate made from a linear-graphite-hybrid (LGH) has also been proposed [5]. They are based on the concept that the reactivity of lithium with the organic electrolyte is reduced by absorbing the lithium within matrix materials such as aluminium and, in consequence, improving the coulombic efficiency of the charge–discharge cycle.

Up to the present, there have been many papers on the electrochemical behavior of lithium-alloying substrates in organic electrolytes. However, the exact relation between the degree of alloy formation and the charge–discharge behavior of the resulting alloy has not yet been clarified. In this paper, we report on an examination of some amorphous alloys containing nickel or cobalt as the main component, and the charge–discharge characteristics of lithium on the alloy substrates. The variations of cycling coulombic efficiency with substrates and electrolyte compositions are discussed with regard to the diffusion behavior of lithium in the amorphous substrate and the deposition rate of lithium from the electrolyte.

---

*Author to whom correspondence should be addressed.

Experimental

The amorphous alloys were $Ni_{70}Al_{10}B_{20}$ and $Co_{70}Al_{10}B_{20}$ (the compositions are in at.%) prepared at Riken, Inc. Ribbons of the alloys (0.5 mm) wide, 0.02 mm thick) were spot-welded to a nickel wire and degreased with acetone in an ultrasonic cleaner. A partly-crystallized alloy was prepared by annealing the amorphous alloy at 500 °C under vacuum. The amorphousness of the alloy was estimated qualitatively by X-ray diffraction (XRD). The alloys, with the exception of 2 cm at the ends which were exposed to the electrolyte, were sealed with Teflon resin.

The electrolyte solvents were propylene carbonate (PC), dimethylsulfoxide (DMSO), and a mixture of the two (1:1 by volume). In some experiments, 1,2-dimethoxyethane (DME) was used as a cosolvent of DMSO. The electrolytic salt was 1 mol dm^{-3} (1 M) of $LiClO_4$, $LiBF_4$, or $LiPF_6$.

The coulombic efficiency of lithium at the alloy substrate was measured by a galvanostatic charge–discharge cycle in a beaker cell [6]. The cycling current was usually 2 mA cm^{-2}, and the amount of charge was 0.2 C cm^{-2} (i.e., 2 mA cm^{-2} × 100 s). The efficiency in each cycle was defined as

$$E_{eff} = (Q_{dis}/Q_{ch}) \times 100 \ [\%] \tag{1}$$

where Q_{dis} and Q_{ch} are the amounts of charge for discharge and charge, respectively. The lithium diffusion coefficient in the solid phase was evaluated by a potential-step method [7]. The electrochemical experiments were carried out at room temperature (16 - 22 °C) in a glove box filled with dry argon.

Results and discussion

The XRD patterns of the alloys showed that the original (as received) $Co_{70}Al_{10}B_{20}$ was almost completely amorphous, and the annealed alloy contained a partially crystallized phase. These are subsequently referred to as Co alloy(a) and Co alloy(c), respectively. The $Ni_{70}Al_{10}B_{20}$ sample (Ni alloy) also consisted of an amorphous phase containing a small amount of a crystallized phase.

Figure 1 shows the coulombic efficiencies of lithium cycled on Co alloy(a) in $LiPF_6$/DMSO, $LiBF_4$/DMSO and $LiClO_4$/DMSO. The efficiency was dependent on the electrolytic salt ($LiPF_6 > LiBF_4 > LiClO_4$). This is in accordance with the cycling behavior on a nickel substrate in DMSO-based electrolytes [8]. The main reason for the efficiency loss during the charge–discharge cycles is probably due to a chemical reaction between the deposited lithium and the electrolyte (solvent and/or salt). The charge–discharge behavior was dependent on the cycling current density. The efficiency decreased significantly at higher current densities (>5 mA cm^{-2}). In the moderately low current region (0.1 - 2.0 mA cm^{-2}), however, the efficiency–cycle profile was scarcely affected by the cycling rate.
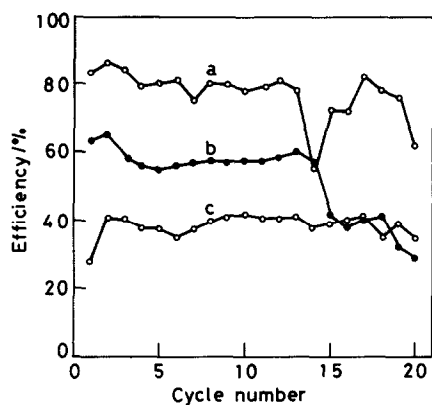
Fig. 1. Lithium cycing efficiency on Co alloy(a) in DMSO containing 1 mol dm^{-3} of LiPF$_6$ (a), LiBF$_4$ (b), and LiClO$_4$ (c), i_{cy} = 2 mA cm^{-2}, Q_{ch} = 0.2 C cm^{-2}.
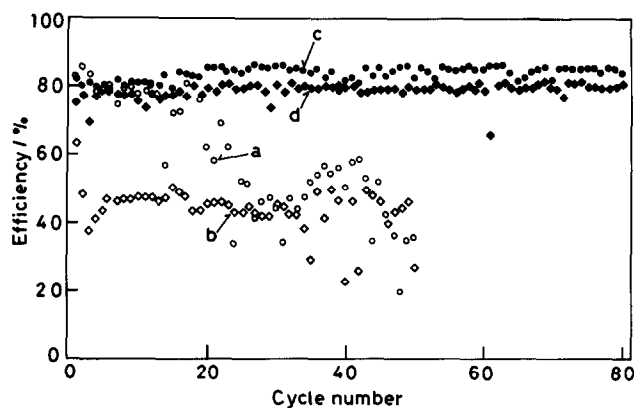

Fig. 2. Lithium cycling efficiency on Co alloy(a) (a, c) and Ni alloy (b, d) in 1 mol dm^{-3} of LiPF$_6$, a, b: DMSO, c, d: DMSO–PC (1:1 by vol.), i_{cy} = 2 mA cm^{-2}, Q_{ch} = 0.2 C cm^{-2}.

The lithium cycling efficiency was improved by mixing DME or PC with DMSO. Figure 2 shows the efficiency variation with cycle number for Co alloy(a) and Ni alloy in LiPF$_6$/DMSO and LiPF$_6$/DMSO–PC(1:1). In both electrolytes, the efficiencies with Co alloy(a) were higher than those with Ni alloy. This trend, other than for relatively low efficiency values, was also observed in other solutions containing LiClO$_4$ or LiBF$_4$. The lithium efficiency with the Ni alloy was fairly low in LiPF$_6$/DMSO, but in LiPF$_6$/DMSO–PC it was relatively high, and it only varied slightly with cycle number. The cell with Co alloy(a) in LiPF$_6$/DMSO showed a high efficiency during initial cycling but it decreased after 15 - 20 cycles. The use of DMSO–PC mixed solvent was effective in keeping the efficiency high even after repeated cycles. The DME–DMSO mixture apparently has a similar effect. Mixed solvent effects were also observed in LiBF$_4$ and LiClO$_4$ solutions [9].

The coulombic efficiency of lithium was also dependent on the substrate alloy. Figure 3 shows efficiency variation with cycle number in LiBF$_4$/
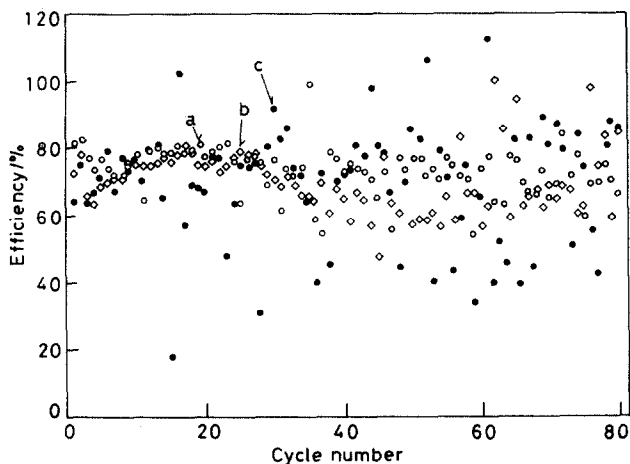
Fig. 3. Lithium cycling efficiency on Co alloy(a) (a), Ni alloy (b) and Co alloy(c) (c) in DMSO–PC(1:1 by vol.) containing 1 mol dm^{-3} of LiBF$_4$, i_{cy} = 2 mA cm^{-2}, Q_{ch} = 0.2 C cm^{-2}.

DMSO–PC. Over the initial 10 cycles, the efficiency did not vary significantly for Co alloy(a), Co alloy(c) and Ni alloy. However, the efficiency with Co alloy(c) varied significantly with cycle number after the 10th cycle. This is probably due to a non-ideal lithium deposition–dissolution process on this substrate. A similar tendency was also observed for the Ni alloy. The efficiency variation order was Co alloy(a) < Co alloy(c) < Ni alloy in LiBF$_4$/DMSO–PC. As shown in Fig. 2, the efficiency variation with cycle number was generally small in LiPF$_6$ solutions, but the efficiency value itself was dependent on the substrate in these electrolytes. The efficiency order tended to be Co alloy(a) > Co alloy(c) > Ni alloy in LiBF$_4$/DMSO–PC.

The difference between the charge–discharge behavior in the substrates, especially the coulombic efficiency and its variation with cycle number, was related to the diffusivity of lithium in the substrate material. The partly crystallized Co alloy(c) had a lower cycleability than Co alloy(a). It is considered that the difference in efficiency between Co alloy(a) and Ni alloy (Fig. 2) may be attributed to the amorphousness of the solid.

Generally, metal substrates spontaneously alloying with lithium show high coulombic efficiencies [10, 11]. The substrates act as a matrix or lithium absorber. The current decay curves for lithium deposition were measured by the potential step method [7]. Typical current–time relations are plotted in Fig. 4. The diffusion constants of the electroactive species are determined from the straight line slopes using the Cottrel eqn. (2):

$$i(t) = FSC_s(D/\pi t)^{1/2} \tag{2}$$

where $i(t)$ is the current at time t; F, the Faraday constant; S, the surface area of the electrode; C_s, the saturated concentration of lithium in the substrate; and D is the diffusion constant. Table 1 summarizes the apparent diffusion constants obtained for the alloys in various electrolytes. In this
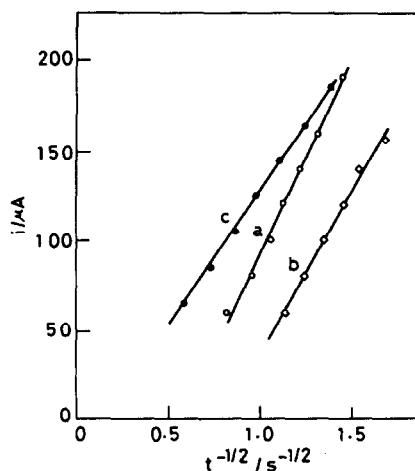
Fig. 4. Current–time relations at Co alloy(a) (a), Ni alloy (b), and Co alloy(c) (c) in DMSO–PC(1:1 by vol.) containing 1 mol dm^{-3} of LiBF$_4$, $E = +10$ mV $vs.$ Li/Li$^+$.

TABLE 1

Apparent diffusion coefficient, D, of lithium in the alloy substrate

Electrolyte	$D/10^{-12}$ cm^2 s^{-1}		
	Ni alloy	Co alloy(a)	Co alloy(c)
LiClO$_4$/DMSO	3.4	6.1	2.3
LiBF$_4$/DMSO	3.6	5.4	2.5
LiClO$_4$/DMSO–PC(1:1)	3.8	5.8	2.5
LiBF$_4$/DMSO–PC(1:1)	3.6	5.5	2.2

case C_s was estimated as 8.7×10^{-3} mol cm^{-3}, which is equivalent to the maximum lithium concentration in the β-phase Li–Al alloy, Li$_{0.38}$Al$_{0.62}$ [11]. As the diffusion process was rate-determining in the solid, the D value was independent of the electrolyte solution. The higher D in the Co alloy than that in the Ni alloy seems to correspond to the higher cycling efficiencies with the Co alloy. The diffusivity in the partly crystallized Co alloy(c) was lower than that in Co alloy(a), which is also in accord with the order of cycling efficiency. On the other hand, the differences in the cycleability between the electrolyte compositions are related to the differences in the deposition–dissolution process, which were mentioned previously. As the deposited lithium reactivity with the electrolyte is probably a main cause of efficiency loss on the substrate, the degree of reactivity determines the cycling efficiency order in different electrolytes.

References

1 Y. Matsuda, M. Morita and H. Katsuma, *Denki Kagaku*, *49* (1981) 537; *J. Electrochem. Soc.*, *130* (1983) 627.

2 K. Yoshimitsu, S. Kitagawa, K. Kajita and T. Manabe, *Ext. Abstr. 26th Battery Symp. in Japan (1A13), Kyoto, 1985*, p. 49.

3 N. Koshiba, H. Hayakawa and K. Momose, *Ext. Abstr. 26th Battery Symp. in Japan (2A05), Kyoto, 1985*, p. 145.

4 M. Ogawa, T. Fuse, T. Kita, T. Kawagoe and T. Matsunaga, *Ext. Abstr. 27th Battery Symp. in Japan (3A06L), Osaka, 1986*, p. 197.

5 K. Inada, K. Ikeda, Y. Sato, A. Itsubo, M. Miyabayashi and H. Yui, *Ext. Abstr. 27th Battery Symp. in Japan (2A085), Osaka, 1986*, p. 97.

6 V. R. Koch and S. B. Brummer, *Electrochim. Acta, 23* (1978) 55.

7 Y. Geronov, P. Zlatinova and G. Staikov, *J. Power Sources, 12* (1984) 155.

8 M. Morita, F. Tachihara and Y. Matsuda, *Electrochim. Acta, 32* (1987) 299.

9 M. Morita and Y. Matsuda, *J. Power Sources, 20* (1987) 299.

10 A. N. Dey, *J. Electrochem. Soc., 118* (1971) 1547.

11 M. Morita, S. Nishikawa and Y. Matsuda, *Denki Kugaku, 53* (1985) 735.